

Spectral change of simulated X-ray photoelectron spectroscopy from graphene to fullerene

Jungpil Kim¹ · Yasuhiro Yamada¹ · Miki Kawai¹ · Takehiro Tanabe¹ · Satoshi Sato¹

Received: 7 March 2015 / Accepted: 1 July 2015 / Published online: 10 July 2015
© Springer Science+Business Media New York 2015

Abstract C1s X-ray photoelectron spectroscopy (XPS) spectra of graphene with two to eight pentagons and fullerene pentagons were simulated using density functional theory calculation. Peak shifts and full width at half maximum (FWHM) of calculated C1s spectra were compared with those of actual C1s spectra. Introduction of up to four isolated pentagons had no influence on shifts of the calculated peak maxima of graphene (284.0 eV), whereas the introduction of six or more pentagons shifted the calculated peak maximum toward low binding energies because the number of connected pentagons increased. The presence of pentagons also influenced FWHMs. Introduction of six pentagons increased the calculated FWHMs from 1.25 to 1.45 eV, whereas introduction of eight or more pentagons decreased the FWHMs. The FWHM reached at 1.15 eV by introducing twelve pentagons (fullerene). These calculated shifts and FWHMs were close to the actual shifts of graphite (284.0 eV) and fullerene (282.9 eV) and FWHMs of graphite (1.25 eV) and fullerene (1.15 eV). Based on the calculated and the actual results, we proposed peak shifts and FWHMs of graphene with the different number of pentagons, which can be utilized for analyzing actual XPS spectra. Proposed FWHMs can be adjusted by measuring actual FWHMs using each device.

Introduction

Graphene has received enormous attention because of various possible applications such as electronic devices and catalyst supports [1]. The presence of pentagons in graphene changes the morphology [2], electronic states [3], and reactivity of graphene [4]. Quantitative information such as the number of pentagons per area (i.e., areal density) in graphene and qualitative information such as closeness of pentagons are essential to understand such electrical and chemical properties.

Pentagons have been analyzed by several methods such as high-resolution transmission electron microscopy (HRTEM) [5] and Raman [6], infrared (IR) [7], and nuclear magnetic resonance (NMR) [8] spectroscopies. For example, pentagons have been directly observed at grain boundaries of graphene and defective structures of reduced graphene oxide by HRTEM [5], but electron irradiation during observation may cause the structural change and prevent from observing correct structures. Raman and IR spectroscopies have been utilized to determine vacancy defects and Stone–Thrower–Wales (STW) defects in graphene [6, 7], but the peaks solely analyzing pentagons have not been reported other than fullerenes. In addition, Raman and IR spectroscopies have disadvantages in quantitative analysis. Conventional solid-state NMR spectroscopy requires the large amount of samples for measurement, which is not suitable for analyzing precious nanomaterials. Thus, it is urgent to develop other analytical techniques.

X-ray photoelectron spectroscopy (XPS) analysis can be one of the suitable techniques to analyze graphene with pentagons quantitatively and qualitatively. Most research groups have separated the main peak of C1s spectra of graphene as sp^2C and sp^3C , and neglected the analysis of detailed states of bonding of graphene. In terms of

Electronic supplementary material The online version of this article (doi:10.1007/s10853-015-9229-0) contains supplementary material, which is available to authorized users.

✉ Yasuhiro Yamada
y-yamada@faculty.chiba-u.jp

¹ Graduate School of Engineering, Chiba University, 1-33 Yayoi, Inage, Chiba 263-8522, Japan

fullerene containing pentagons, the peak position of C1s spectra has been reported, but the peak originating from pentagons of fullerenes has not been separated from hexagons because all pentagons connect with hexagons [9–11]. Because of the difficulty to synthesize such reference compounds currently, computational simulation is necessary as one of the tools to investigate the structure clearly.

Computational simulations of XPS spectra have been recently utilized to clarify the defective structures of graphene-related materials [12–20]. Since Proctor and Sherwood [13] as well as Boutique et al. [14] have started computational analyses of functional groups on carbon materials in the 1980s, several groups have reported assignments of defective structures of graphene-related materials using calculation [15–20]. Until the present, XPS analysis of pentagons on graphene has not been reported except three papers [12, 20, 21] to the best of our knowledge. For example, point defects including one pentagon in graphene have been analyzed and the peak originating from the pentagon was shifted to -0.8 eV from a peak originating from carbon atoms on hexagons [12]. As another example, peak shifts originating from carbon atoms on pentagon in single vacancies (from -1.10 to -0.37 eV), double vacancies (from -1.18 to -0.34 eV), and STW defects (-0.94 eV) from a sp^2C – sp^2C peak of graphene have been reported [20]. These works showed only the peak shifts originating from either one or two pentagons in graphene, and influences of the number and closeness of pentagons on peak shifts as well as the full width at half maximum (FWHM) were not mentioned.

Our group has demonstrated the effects of defects such as functional groups and STW defects on FWHMs and shifts of XPS spectra [21, 22]. Electron-withdrawing groups such as C=O and C–CN have large effects on shifts as well as FWHMs of main peaks consisting of sp^2C – sp^2C . Pentagons have a similar role to C=O and C–CN because of their electron-withdrawing nature [23]. It is possible that the presence of pentagons also affects the shifts of main peaks as well as FWHMs.

In this work, the effects of the number and the position of introduced pentagons on C1s shifts and FWHMs were analyzed using computational simulation of C1s XPS spectra. In addition, influences of connectivity of pentagons in graphene on C1s spectra have been studied.

Experimental

Computation

Graphene terminated with hydrogen atoms on zigzag and armchair edges ($C_{100}H_{26}$) was utilized (Fig. 1) as a basic structure in this work. The reason for selecting $C_{100}H_{26}$ as

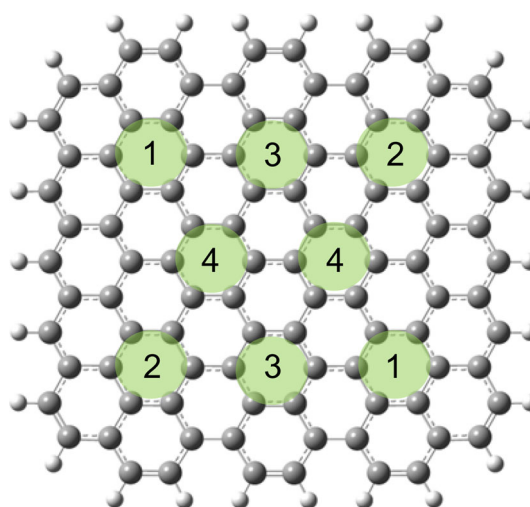


Fig. 1 Positions of introduced pentagons and the numbering of the positions in graphene terminated with hydrogen atoms. Two pentagons: Position 1. Four pentagons: Positions 1 and 2. Six pentagons: Positions 1, 2, and 3. Eight pentagons: Positions 1, 2, 3, and 4 (Color figure online)

the basic structure is shown in Fig. S1 (Supplementary material: SM). The introduced positions of pentagons and the numbering of the positions are indicated in the structure (Fig. 1). All of the structures used in this work are shown in Fig. 2. Zero (Fig. 2a), two (Fig. 2b), four (Fig. 2c), six (Fig. 2d), and eight (Fig. 2e) pentagons were introduced in the basal plane of graphene. Peak positions and FWHMs of XPS spectra of isolated pentagons such as two (Fig. 2b) and four (Fig. 2c) pentagons in graphene and connected pentagons such as six (Fig. 2d) and eight (Fig. 2e) pentagons in graphene were estimated to determine the existence of isolated pentagons and connected pentagons. For comparison, C_{60} fullerene with twelve pentagons (Fig. 2f) was also calculated. These structures include mainly three types of carbon atoms such as C1 (sp^2C – sp^2C on hexagons), C2 (sp^2C –H), and C3 (carbon atoms on pentagons).

All of the following calculations were conducted using B3LYP/6-31g(d) integral = grid = ultrafine of Gaussian 09 [24]. After the structures were optimized using the keyword of opt, population analyses for simulated XPS spectra using the keyword of pop = full gfprint were conducted. Charge of the structures was set as either 0 or 2, but the charge was basically equal to 0 unless stated. Spin multiplicity was set as 1 for all calculations. Binding energies of these model structures were obtained from the orbital energy, which was calculated from the highest occupied molecular orbital (HOMO) level to each orbital.

It has been known that the initial and final state effects have an influence on the XPS spectra [25–27]. However, we simulated the XPS spectra using only the initial state effect by applying the scaling factor to the spectra in this work because of the simplicity of this method with good

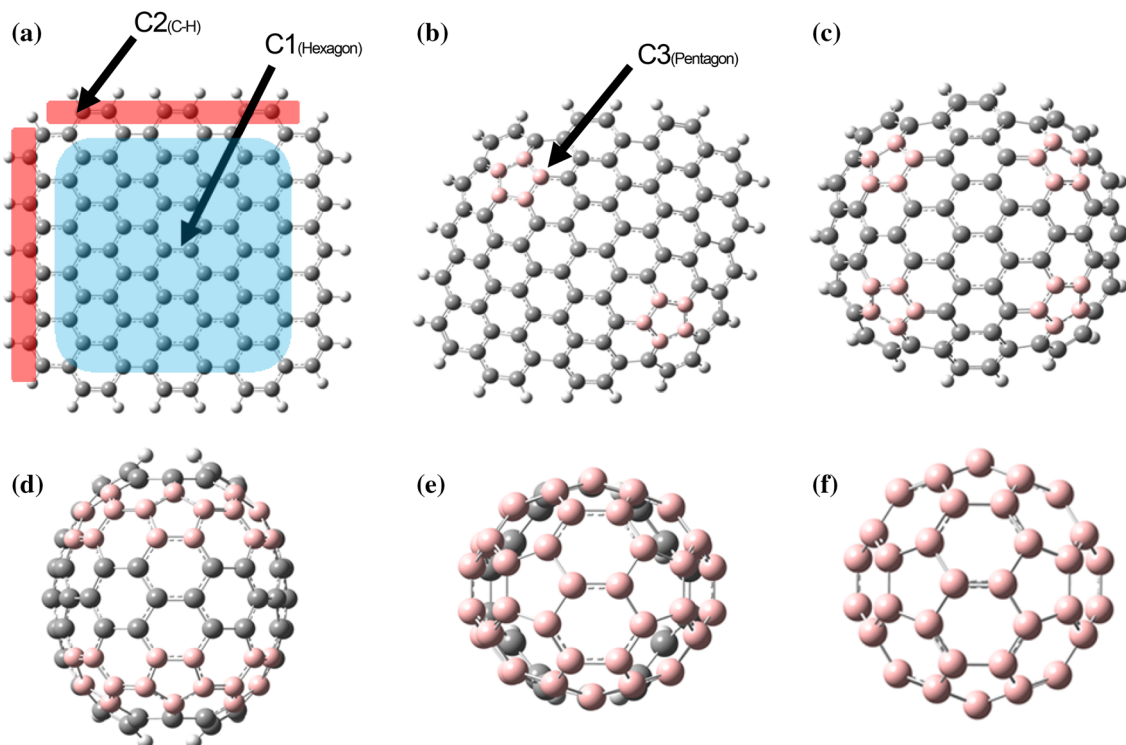


Fig. 2 Optimized structures of graphene, pentagon-containing graphene, and fullerene. All the edges were terminated with hydrogen atoms (white sphere). C1 is carbon atoms on hexagons which bonded with carbon atoms. C2 is carbon atoms bonded with hydrogen atoms.

C3 is carbon atoms on pentagons (pink spheres). **a** Graphene terminated with hydrogen atoms. **b** Two pentagons. **c** Four pentagons. **d** Six pentagons. **e** Eight pentagons. **f** Twelve pentagons without hydrogen atoms (fullerene) (Color figure online)

correlation between actual and calculated results [21, 22]. For simulating C1s spectra using the calculated binding energy, the scaling factor of 1.038, obtained from the actual value of graphite (284.0 eV from valence band edge) divided by the calculated value of graphene terminated with hydrogen atoms (273.7 eV from HOMO level), was multiplied to all of the calculated binding energies to compensate for the difference between the calculated and the actual binding energies instead of the application of the final state effects.

The number of orbitals was counted every 0.05 eV to simulate C1s spectra (Fig. S2, SM). Furthermore, modified asymmetric Voigt-type lineshape [28] was applied to obtain simulated XPS spectra which resemble actual XPS spectra (Fig. S3a, b, SM). Different values of ratio of Lorentzian function to Gaussian function (m) calculated by the following equation were applied to XPS spectra for the better fitting of actual spectra (Figs. 3 and S3c).

$$m = \frac{\text{Lorentzian function}}{\text{Lorentzian function} + \text{Gaussian function}} \quad (1)$$

Different values of asymmetry factor (α) [28] were also applied to XPS spectra for the better fitting of actual spectra (Figs. 3 and S3c). All of the maximum intensities

of C1s spectra were adjusted at 1.0 for fair comparisons (Fig. 3). The number of electrons of carbon atoms in each structure was obtained using the Mulliken population analysis. The averaged numbers of electrons were obtained by adding the number of electron (6.000) for carbon atoms to the negative value of Mulliken charge.

XPS analysis

Graphite powder (SP270, particle size: 4 μm , Brunauer–Emmett–Teller (BET)-specific surface area: 265 $\text{m}^2 \text{g}^{-1}$) was provided from Nippon Graphite Industries, Ltd in Japan. This graphite consists of ca. ten layers of graphene as geometrically calculated from the BET-specific surface area. In this work, graphene terminated with hydrogen atoms (Fig. 2a) was utilized for the calculated XPS analysis, but graphite containing ten layers of graphene was used for actual XPS analysis. It was because metal substrates under graphene synthesized by a chemical vapor deposition (CVD) method have an effect on the work function of graphene (4.20–4.55 eV) [29, 30], indicating that variation of peak shifts of XPS spectra can be generated depending on the types of substrates. It is necessary to adjust the peak top of XPS spectra for measurement of

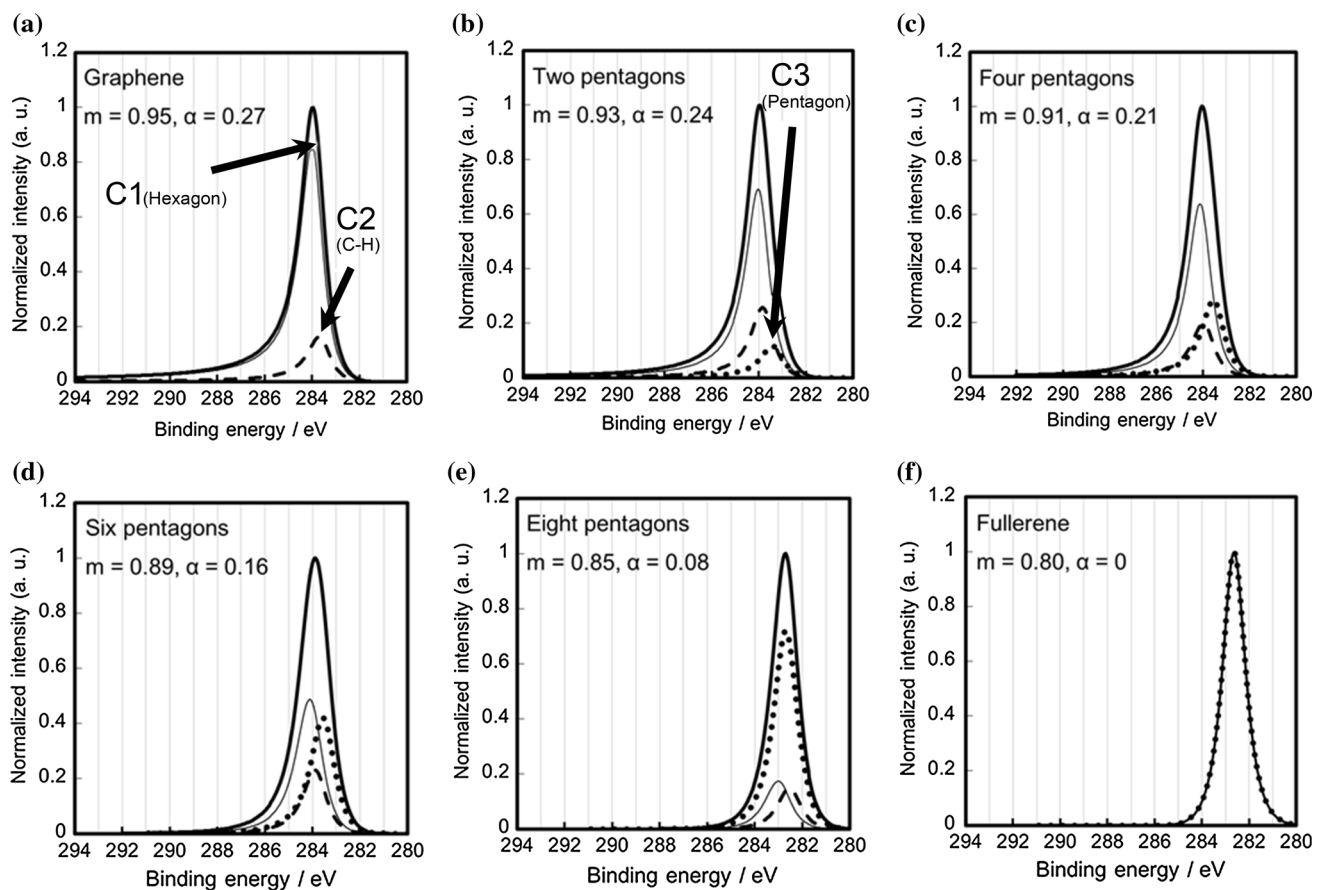


Fig. 3 Simulated C1s XPS spectra of structures shown in Fig. 2 using asymmetric Voigt-type lineshapes. Simulated original spectra are shown as *bold lines*. Peaks originating from carbon atoms on hexagons which bonded with carbon atoms (C1), carbon atoms bonded with hydrogen atoms (C2), and carbon atoms on pentagons

(C3) are shown as *thin, dashed, and dotted lines*, respectively. **a** Graphene terminated with hydrogen atoms. **b** Two pentagons. **c** Four pentagons. **d** Six pentagons. **e** Eight pentagons. **f** Twelve pentagons without hydrogen atoms (fullerene). Values of m and α (Fig. S3c, SM) were applied to each spectrum

graphene depending on the types of substrates. Thus, we analyzed graphite instead of analyzing graphene on various substrates. Fullerene (C_{60}) was purchased from Kanto Chemical, Ltd. in Japan.

XPS analysis (AXIS ULTRA DLD, Shimadzu Corp.) was conducted using X-ray gun of Mg at 10 mA and 10 kV and pass energy of 40 eV. Samples were placed on conductive tapes (3 M X-7001) for XPS analysis. The binding energies at peak maxima of C1s spectra of graphite and fullerenes were obtained after adjusting energies at valence band edge to 0 eV. As another method, $Au4f_{7/2}$ of gold nano powder (99.9 %, <100 nm, Sigma-Aldrich Corp.), was set at 83.8 eV [31]. Two methods to adjust binding energy were described above, but adjustment of energies at valence band edge to 0 eV was basically used in this work unless stated. The modified asymmetric Voigt-type lineshape [28] was applied to separate the waveform of XPS spectra. All of the maximum intensities of C1s spectra were adjusted to 1.0.

Results and discussion

Figure 3a–f shows C1s spectra simulated for the structures depicted in Fig. 2a–f. The peak maxima originating from C1 (a thin line) and C2 (a dashed line) in Fig. 3a were at 284.0 and 283.7 eV, respectively. The peak maximum of C2 was lower than that of C1 in binding energy because hydrogen atoms donate electrons to carbon atoms of C2 (Fig. S4, SM) [21, 22]. The peak maximum of C3 in graphene with two pentagons was at 283.4 eV (a dotted line in Fig. 3b), whose binding energy was the lowest among those of C1, C2, and C3 because of electron-withdrawing nature of pentagons (Fig. S5, SM). In Table 1 and Fig. 3, the binding energies of peak maxima of C3 for graphene with two, four, and six pentagons were the lowest among peak maxima of C1, C2, and C3 of each spectrum (Fig. 3b–d), but the binding energy of the peak maximum of C2 for graphene with eight pentagons (282.6 eV in Fig. 3e) was lower than that of C3 (282.7 eV in Fig. 3e). This change

Table 1 Peak shifts and FWHMs of C1s spectra

Number of pentagons			0	2	4	6	8	12
Ratio of the number of carbon atoms (C1:C2:C3)			100:26:0	60:22:10	46:18:20	32:14:30	10:8:40	0:0:60
Empirical data from a reference [32]	Whole C1s spectrum	Peak top (eV)	284.3 (Graphite)	–	–	–	–	284.7
		FWHM (eV)	1.25	–	–	–	–	1.15
Simulated data from a reference [32]	Whole C1s spectrum	Peak top (eV)	289.7–290.1 (Pyrene)	–	–	–	–	290.5
		FWHM (eV)	1.25	1.30	1.35	1.45	1.25	1.15
Empirical data in this work	Whole C1s spectrum	Peak top (eV)	284.0	–	–	–	–	282.9
		FWHM (eV)	1.25	–	–	–	–	1.15
Simulated data in this work	Whole C1s spectrum (C1 + C2 + C3)	Peak top (eV)	284.0	284.0	284.0	283.9	282.7	282.7
		FWHM (eV)	1.25	1.30	1.35	1.45	1.25	1.15
	C1 + C3 (Hexagon + Pentagon)	Peak top (eV)	–	284.0	284.0	283.9	282.8	–
		FWHM (eV)	–	1.25	1.45	1.55	1.25	–
	C1 (Hexagon)	Peak top (eV)	284.0	283.9	283.9	283.9	283.0	–
		Peak shift from C1 of graphene to C1 (eV)	0	0.1	0.1	0.1	–1.0	–
		FWHM (eV)	1.15	1.20	1.15	1.30	1.20	–
	C2 (C–H)	Peak top (eV)	283.7	283.9	284.0	283.9	282.6	–
		Peak shift from C1 to C2 (eV)	–0.3	–0.2	–0.1	–0.2	–0.4	–
		FWHM (eV)	1.15	1.20	1.20	1.15	1.15	–
	C3 (Pentagon)	Peak top (eV)	–	283.4	283.6	283.6	282.7	–
		Peak shift from C1 to C3 (eV)	–	–0.7	–0.5	–0.5	–0.3	–
FWHM (eV)		–	1.20	1.15	1.20	1.15	–	
Averaged number of electrons of one carbon atom on one pentagon ^a			–	6.066	6.060	6.034	6.008	–

^a Averaged number of electrons of one carbon atom on one pentagon: the calculated method is shown in SM

was induced by the connection of all eight pentagons in graphene (Fig. 2e) and the decrease in the number of electrons on carbon atoms (Table 1; Fig. S6, SM).

The peak maximum of calculated C1s spectra of graphene (284.0 eV) was slightly shifted to 283.9 eV by introducing six pentagons, and the peak maximum was dramatically shifted to lower binding energy as the number of connected pentagons increased. The peak maximum reached up to 282.7 eV by introducing twelve pentagons (fullerene) (Figs. 2f and 3f; Table 1). These tendencies were well matched with results simulated without C2 (C1 + C3 in Table 1). Actual peak maxima of C1s spectra of graphite and fullerenes analyzed in this work were 284.0 and 282.9 eV from valence band edge, respectively (Fig. 5). The actual peak shift of the C1s spectrum of fullerene deviated from that of graphite was –1.1 eV, whereas the calculated peak shift of the C1s spectrum of fullerene deviated from that of graphene was –1.3 eV (Table 1).

The reported empirical binding energy of the peak maximum of a C1s spectrum for graphite (284.3 eV), on the other hand, was lower than that for C₆₀ (284.7 eV) (Table 1) [32]. Similarly, the reported calculated binding

energy of the peak maximum of the whole C1s spectrum for pyrene (from 289.7 to 290.1 eV), which was utilized as a substitute of graphite in the paper, was lower than that of C₆₀ (290.5 eV) [32]. The opposite tendency between our results and reported values [32] can be explained by the difference of standards. In this work, the peak maxima of empirical C1s spectra of graphite and C₆₀ using Au4f_{7/2} as a standard were 284.3 and 284.6 eV, respectively. The peak maxima of calculated C1s spectra of graphene and C₆₀ using vacuum level as a standard in this work were 284.3 and 285.1 eV, respectively. Thus, the reported data (284.3 eV for graphite and 284.7 for fullerene in [32]) were similar to our actual data using Au and calculated data using vacuum level. However, we utilized the valence band edge as a standard (Fig. 5) instead of Au to eliminate possible various factors.

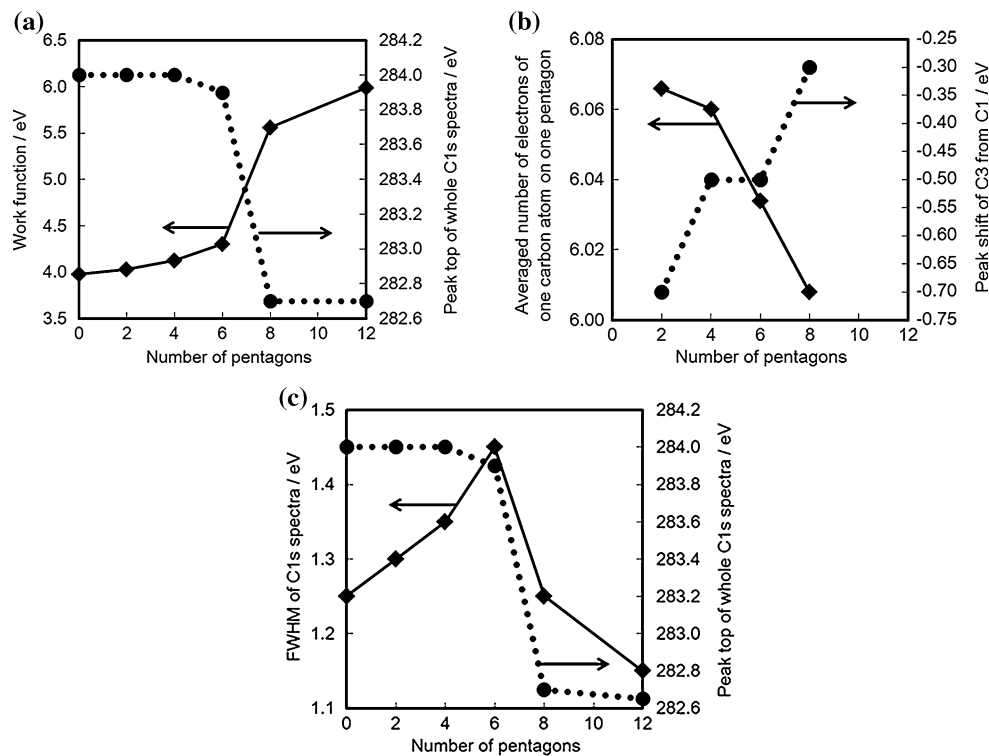
Several groups have reported that the work functions of graphite and C₆₀ are 4.73–4.80 and 6.16–6.50 eV [33, 34], respectively. In this work, the calculated work functions, which were determined from energy differences between HOMO level [35] and vacuum level, were 3.98, 4.03, 4.13, 4.30, 5.56, and 5.99 eV for graphene with zero (graphene),

Table 2 Comparison of work function between this work and reported data

Number of pentagons	0	2	4	6	8	12
Ratio of the number of carbon atoms (C1:C2:C3)	100:26:0	60:22:10	46:18:20	32:14:30	10:8:40	0:0:60
Calculated work function in this work ^a (eV)	3.98	4.03	4.13	4.30	5.56	5.99
Empirical work function from a reference (eV) [33]	4.73 (Graphite)	–	–	–	–	6.16
Empirical work function from a reference (eV) [34]	4.80 (Graphite)	–	–	–	–	6.50

^a Work function: energy difference between HOMO level and vacuum level

Fig. 4 Dependence of physical properties on the number of pentagons. **a** Dependence of work functions and peak maxima of whole C1s spectra on the number of pentagons. **b** Dependence of averaged numbers of electrons of one carbon atom on one pentagon and peak shifts of C3 from C1 on the number of pentagons. **c** Dependence of FWHMs and peak maxima of C1s spectra on the number of pentagons



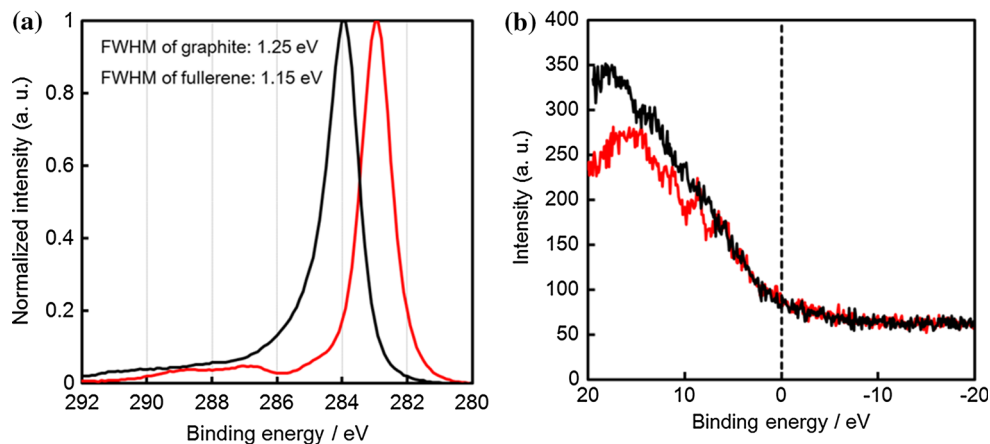
two, four, six, eight, and twelve (fullerene) pentagons, respectively (Table 2). Previously explained negative shifts of the peak maximum of whole C1s spectra were well correlated with the increment of these work functions as the number of pentagons increased (Table 2; Fig. 4a), because valence band edge becomes close to the atomic nucleus and the binding energy of the C1s peak of graphene with pentagons becomes smaller than that of graphene without pentagons.

Table 1 shows peak shifts from C1 of graphene without pentagons to C1 of graphene with pentagons, which is written as “Peak shift from C1 of graphene to C1”. It also shows peak shifts from C1 to C2 as well as peak shifts from C1 to C3. C1 was negatively shifted from 284.0 to 283.0 eV as the number of pentagons increased from zero to eight. The peak shifts of C2 for graphene with and without pentagons ranged from -0.1 to -0.4 eV,

indicating that the shift from C1 to C2 was small. The peak shifts of C3 for graphene with two, four, six, and eight pentagons from C1 were -0.7 , -0.5 , -0.5 , and -0.3 eV, respectively (Table 1; Fig. 3). The increment of peak shifts from C1 to C3, i.e., from -0.7 to -0.3 eV, can be explained by an averaged number of electrons of one carbon atom on one pentagon. The averaged numbers of electrons of one carbon atom on one pentagon were 6.066, 6.060, 6.034, and 6.008 in graphene with two (Fig. S5, SM), four, six, and eight pentagons, respectively (Table 1). Especially, connection of pentagons reduced the number of electrons (Fig. S6, SM) and caused the positive peak shifts of C3 (Fig. 4b).

The number of pentagons in graphene also had an influence on FWHMs of C1s spectra in addition to the shift. Calculated FWHMs of whole C1s spectra of graphene (1.25 eV for graphene including peaks originated from C–

Fig. 5 Actual C1s XPS spectra and spectra at valence band edge of graphite and fullerene. **a** C1s spectra. **b** Spectra at valence band edge. *Black line* graphite. *Red line* fullerene (Color figure online)



H bonding and 1.15 eV for graphene excluding peaks originated from C–H bonding) and fullerenes (1.15 eV) in Table 1 and Fig. 4c were equal to actual FWHMs of whole C1s spectra of graphite (1.25 eV) and fullerenes (1.15 eV) in Fig. 5a. FWHMs increased to 1.30, 1.35, and 1.45 eV by introducing two, four, and six pentagons in graphene, respectively (Table 1; Fig. 4c). The reason for the small FWHMs of the calculated and actual C1s spectra of graphene (1.25 eV) and fullerenes (1.15 eV), compared with those of graphene with two to eight pentagons, is the presence of either similar or same states of C–C bonding, respectively. For example, graphene terminated with hydrogen atoms contains only two types of carbon atoms such as hexagonal sp^2C-sp^2C (C1) and sp^2C-H (C2). C1 and C2 are close to each other. Fullerene contains only one type of pentagonal sp^2C-sp^2C (C3). The increment of pentagons increased the presence of different states of C–C bondings and FWHMs became wide similar to our previously reported results of FWHMs of C1s spectra for graphene with oxygen- and nitrogen-containing functional groups [21, 22]. The FWHM of whole C1s XPS spectra (C1 + C2 + C3) basically depended on the degree of the calculated peak shifts of C1, C2, and C3 spectra as well as the ratios among the numbers of carbon atoms of C1, C2, and C3 (Fig. 3). Especially, the ratio between the number of carbon atoms with the highest binding energy (C1) and that with the lowest binding energy (C3) mainly influenced FWHMs. The number of carbon atoms of C2 is less important than those of C1 and C3. The ratio between C1 and C3 of graphene with six pentagons was close to each other (C1:C3 = 32:30) and this specific ratio increased FWHMs significantly.

Figure 6 and Table 3 show proposed FWHMs and peak maxima of whole C1s spectra, which can be utilized for actual XPS analysis. Actual measured results (Fig. 5a) were merged with calculated results (Fig. 4c; Table 1) to obtain proposed peak maxima accurately (Fig. 6; Table 3). In the analysis of

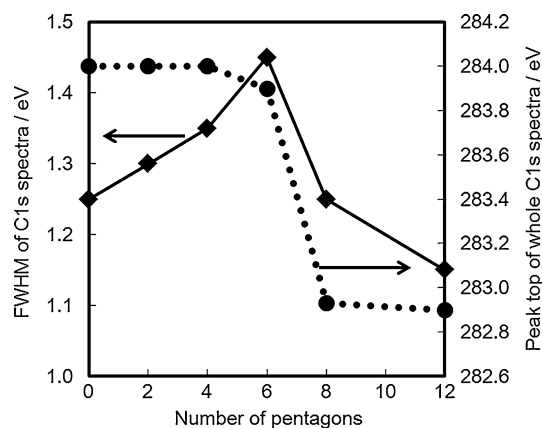


Fig. 6 Proposed FWHMs and peak maxima of whole C1s spectra of graphene including zero to eight pentagons and fullerene. The peak maxima of actual spectra of graphite and fullerene in Fig. 5 were utilized for adjustment. This figure can be utilized even with different FWHMs influenced by the types of the devices by adjusting the FWHMs of calculated C1s spectra to those of actual C1s spectra of fullerene and graphite for each device

actual measured results, the valence band edge of graphite and C_{60} was set as 0 eV (Fig. 5b) for fair comparison between the peak positions of C1s spectra of graphite and C_{60} . Introduction of six pentagons increased the proposed FWHM up to 1.45 eV (Fig. 6; Table 3), and it slightly shifted the proposed peak maximum from 284.0 eV to a low binding energy of 283.9 eV. Introduction of eight pentagons decreased the proposed FWHM compared to six pentagons and shifted the proposed peak maximum to 282.9 eV (Fig. 6; Table 3). The binding energy is high for graphene with zero to six pentagons (from 284.0 to 283.9 eV) and became low by introducing eight pentagons or more (282.9 eV). By separating Fig. 6 into two regions such as below and above six pentagons, the number and the position of pentagons can be determined using FWHMs and peak shifts. For example, a C1s spectrum with 284.0 eV of peak position and 1.30 eV of FWHM indicates

Table 3 Proposed peak shifts and FWHMs of C1s spectra

Number of pentagons	0 (graphene) ^a	2 ^b	4 ^b	6 ^b	8 ^b	12 (fullerene) ^a
Whole C1s spectrum (C1 + C2 + C3)						
Peak top (eV)	284.0	284.0	284.0	283.9	282.9	282.9
FWHM (eV)	1.25	1.30	1.35	1.45	1.25	1.15

^a Peak shifts and FWHMs of XPS spectra of graphene and fullerene were actually measured

^b Proposed peak shifts and FWHMs of XPS spectra of graphene with two, four, six, and eight pentagons were calculated by merging calculated results (Fig. 4c; Table 1) and experimental results (Fig. 5)

existence of two isolated pentagons in graphene, which contains 11 % of carbon atoms on pentagons in graphene with hydrogen atoms (C1:C2:C3 = 60:22:10).

Graphene with one STW defect was also simulated (Fig. S7; Table S1, SM) because the STW defect is one of the well-known defect observed in graphene. The peak top of normal graphene (284.0 eV) (Table 1) increased to 284.2 eV by introducing one STW defect in graphene (Table S1) because of the decrement of the work function (Tables 2 and S1). The FWHM of normal graphene (1.25) (Table 1) increased to 1.40 eV (Table S1) by introducing one STW defect because of the increment of different states of C–C bondings.

Conclusion

Introduction of pentagons in graphene influenced the peak shifts and FWHMs of calculated C1s spectra. The binding energy of the peak maximum of calculated C1s spectra originated from carbon atoms on pentagons was lower than that originating from carbon atoms on hexagons because of electron-withdrawing nature of the pentagons. Introduction of six or more pentagons shifted the peak maximum of simulated spectra of graphene to low binding energy and reached the lowest binding energy by introducing twelve pentagons (fullerene). The negative peak shifts of the calculated C1s spectra related to the increment of the work function. The FWHM of a C1s spectrum of graphene (1.25 eV) increased up to 1.45 eV as the number of pentagons increased up to six because the number of different states of carbon–carbon bondings was maximized. The FWHM decreased down to 1.15 eV by introducing twelve pentagons (fullerene). These results indicate that the number and the position of pentagons in graphene can be estimated by analyzing the FWHMs and the peak shifts of C1s spectra. The FWHMs of graphene and fullerene are different depending on the types of measured XPS devices, but the FWHMs of graphene with pentagons can be easily adjusted by measuring actual FWHMs of graphite and fullerene.

Acknowledgements Acknowledgments are made to Mr. Shingo Kubo at the Kagoshima University in Japan for measuring samples by XPS. Graphite was provided by Nippon Graphite Industries, Ltd.

Funding This study was funded by the Japan Society for the Promotion of Science (JSPS) KAKENHI (Grant Number 26820348).

Conflict of interest Yasuhiro Yamada has received a research grant from the Japan Society for the Promotion of Science (JSPS) and received graphite from Nippon Graphite Industries, Ltd.

References

- Huang C, Li C, Shi G (2012) Graphene based catalysts. *Energy Environ Sci* 5:8848–8868
- An B, Fukuyama S, Yokogawa K, Yoshimura M, Egashira M, Korai Y, Mochida I (2001) Single pentagon in a hexagonal carbon lattice revealed by scanning tunneling microscopy. *Appl Phys Lett* 78:3696–3698
- Tamura R, Tsukada M (1994) Disclinations of monolayer graphite and their electronic states. *Phys Rev B* 49:7697–7708
- Dubois SM, Lopez-Bezanilla A, Cresti A, Triozon F, Biel B, Charlier JC, Roche S (2010) Quantum transport in graphene nanoribbons: effects of edge reconstruction and chemical reactivity. *ACS Nano* 4:1971–1976
- Erickson K, Erni R, Lee Z, Alem N, Gannett W, Zettl A (2010) Determination of the local chemical structure of graphene oxide and reduced graphene oxide. *Adv Mater* 22:4467–4472
- Popov VN, Henrard L, Lambin P (2009) Resonant Raman spectra of graphene with point defects. *Carbon* 47:2448–2455
- Rocquefelte X, Rignanese GM, Meunier V, Terrones H, Terrones M, Charlier JC (2004) How to identify haeckelite structures: a theoretical study of their electronic and vibrational properties. *Nano Lett* 4:805–810
- Gakh AA, Romanovich AY, Bax A (2003) Thermodynamic rearrangement synthesis and NMR structures of C₁, C₃, and T isomers of C₆₀H₃₆. *J Am Chem Soc* 125:7902–7906
- Wohlers M, Bauer A, Rühle TH, Neitzel F, Werner H, Schlögl R (1997) The dark reaction of C₆₀ and of C₇₀ with molecular oxygen at atmosphere pressure and temperatures between 300 and 800 K. *Fuller Sci Technol* 5:49–83
- Zhu Y, Yi T, Zheng B, Cao L (1999) The interaction of C₆₀ fullerene and carbon nanotube with Ar ion beam. *Appl Surf Sci* 137:83–90
- Kim J, Yamada Y, Suzuki Y, Ciston J, Sato S (2014) Pyrolysis of epoxidized fullerenes analyzed by spectroscopies. *J Phys Chem C* 118:7076–7084
- Barinov A, Malcioğlu OB, Fabris S, Sun T, Gregoratti L, Dalmglio M, Kiskinova M (2009) Initial stages of oxidation on

- graphitic surfaces: photoemission study and density functional theory calculations. *J Phys Chem C* 113:9009–9013
13. Proctor A, Sherwood PMA (1982) X-ray photoelectron spectroscopic studies of carbon fiber surfaces. I. Carbon fiber spectra and the effects of heat treatment. *J Electron Spectrosc Relat Phenom* 27:39–56
 14. Boutique JP, Verbist JJ, Fripiat JG, Delhalle J, Pfister-Guillouzo G, Ashwell GJ (1984) 3,5,11,13-Tetraazacycl [3.3.3] azine: theoretical (ab initio) and experimental (X-ray and ultraviolet photoelectron spectroscopy) studies of the electronic structure. *J Am Chem Soc* 106:4374–4378
 15. Casanovas J, Ricart JM, Rubio J, Illas F, Jimenez-Mateos JM (1996) Origin of the large N1s binding energy in X-ray photoelectron spectra of calcined carbonaceous materials. *J Am Chem Soc* 118:8071–8076
 16. Souto S, Pickholz M, dos Santos MC, Alvarez F (1998) Electronic structure of nitrogen–carbon alloys (a-CN_x) determined by photoelectron spectroscopy. *Phys Rev B* 57:2536–2540
 17. Ohta R, Lee KH, Saito N, Inoue Y, Sugimura H, Takai O (2003) Origin of N1s spectrum in amorphous carbon nitride obtained by X-ray photoelectron spectroscopy. *Thin Solid Films* 434:296–302
 18. Kim S, Zhou S, Hu Y, Acik M, Chabal YJ, Berger C, de Heer W, Bongiorno A, Riedo E (2012) Room-temperature metastability of multilayer graphene oxide films. *Nat Mater* 11:544–549
 19. Zhang W, Carravetta V, Li Z, Luo Y, Yang J (2009) Oxidation states of graphene: insights from computational spectroscopy. *J Chem Phys* 131:244505
 20. Susi T, Kaukonen M, Havu P, Ljungberg MP, Ayala P, Kauppinen EI (2014) Core level binding energies of functionalized and defective graphene. *Beilstein J Nanotechnol* 5:121–132
 21. Yamada Y, Yasuda H, Murota K, Nakamura M, Sodesawa T, Sato S (2013) Analysis of heat-treated graphite oxide by X-ray photoelectron spectroscopy. *J Mater Sci* 48:8171–8198. doi:10.1007/s10853-013-7630-0
 22. Yamada Y, Kim J, Matsuo S, Sato S (2014) Nitrogen-containing graphene analyzed by X-ray photoelectron spectroscopy. *Carbon* 70:59–74
 23. Zhou KG, Zhang YH, Wang LJ, Xie KF, Xiong YQ, Zhang HL, Wang CW (2011) Can azulene-like molecules function as substitution-free molecular rectifiers? *Phys Chem Chem Phys* 13:15882–15890
 24. Frisch MJ, Trucks GW, Schlegel HB et al (2009) Gaussian 09, Revision D.01. Gaussian, Inc., Wallingford
 25. Bagus PS, Ilton ES, Nelin CJ (2013) The interpretation of XPS spectra: insights into materials properties. *Surf Sci Rep* 68:273–304
 26. Bagus PS, Illas F, Pacchioni G, Parmigiani F (1999) Mechanisms responsible for chemical shifts of core-level binding energies and their relationship to chemical bonding. *J Electron Spectrosc Relat* 100:215–236
 27. Bellafont NP, Illas F, Bagus PS (2015) Validation of Koopmans' theorem for density functional theory binding energies. *Phys Chem Chem Phys* 17:4015–4019
 28. Kojima I, Fukumoto N, Kurahashi M (1986) Analysis of X-ray photoelectron spectrum with asymmetric Gaussian-Lorentzian mixed function. *Bunseki Kagaku* 35:T96–T100
 29. Yang S, Zhou P, Chen L, Sun Q, Wang P, Ding S, Jiang A, Zhang DW (2014) Direct observation of the work function evolution of graphene-two-dimensional metal contacts. *J Mater Chem C* 2:8042–8046
 30. Kwon KC, Choi KS, Kim SY (2012) Increased work function in few-layer graphene sheets via metal chloride doping. *Adv Funct Mater* 22:4724–4731
 31. Ikeo N, Iijima Y, Niimura N, Sigematsu M, Tazawa T, Matsumoto (1991) Handbook of X-ray photoelectron spectroscopy. JEOL, Tokyo, p 196
 32. Endo K, Matsumoto D, Takagi Y, Shimada S, Ida T, Mizuno M, Goto K, Okamura H, Kato N, Sasakawa K (2008) X-ray photoelectron spectral analysis for carbon allotropes. *J Surf Anal* 14:348–351
 33. Li WY, Ibrahimi AA, Goto K, Shimizu R (2005) The absolute AES is coming; work functions and transmission of CMA. *J Surf Anal* 12:109–112
 34. Shiraiishi M, Ata M (2001) Work function of carbon nanotubes. *Carbon* 39:1913–1917
 35. Briggs D, Grant JT (2003) Surface analysis by Auger and X-ray photoelectron spectroscopy. IM Publications and Surface Spectra Ltd., Manchester, p 39